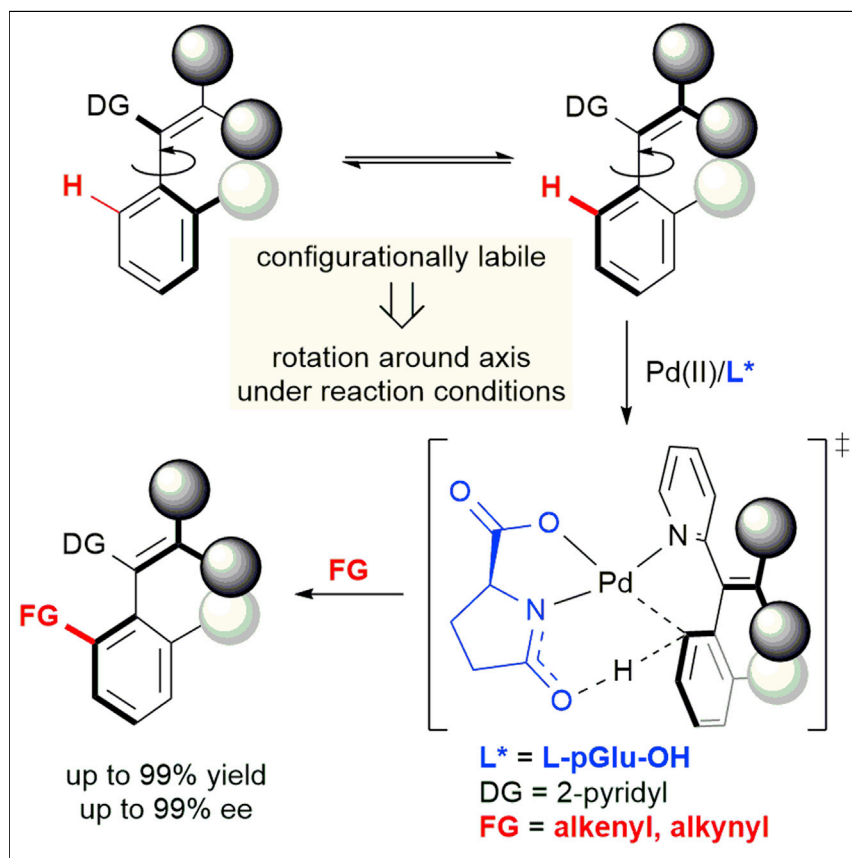


Article

Atroposelective Synthesis of Axially Chiral Styrenes via an Asymmetric C–H Functionalization Strategy



An asymmetric C–H functionalization strategy with L-pGlu-OH as chiral ligand has been developed for the atroposelective synthesis of styrene atropisomers with open-chained alkene. The strategy allows quick access to a wide range of enantio-enriched axially chiral styrenes in high yields and enantioselectivities. The axially chiral styrene-derived chiral acids have been demonstrated to be an efficient type of chiral ligands in Co(III)-catalyzed enantioselective C–H amidation reactions.

Liang Jin, Qi-Jun Yao, Pei-Pei Xie, ..., Ye-Qiang Han, Xin Hong, Bing-Feng Shi

hxchem@zju.edu.cn (X.H.)
bfshi@zju.edu.cn (B.-F.S.)

HIGHLIGHTS

Highly atroposelective synthesis of axially chiral styrenes

L-pyroglutamic acid as an inexpensive and catalytic chiral ligand

Chiral styrene-type acid as ligand in Co-catalyzed enantioselective C–H amidation

A ligand deceleration effect (LDE) in this reaction

Article

Atroposelective Synthesis of Axially Chiral Styrenes via an Asymmetric C–H Functionalization Strategy

Liang Jin,^{1,2} Qi-Jun Yao,^{1,2} Pei-Pei Xie,^{1,2} Ya Li,¹ Bei-Bei Zhan,¹ Ye-Qiang Han,¹ Xin Hong,^{1,*} and Bing-Feng Shi^{1,3,*}

SUMMARY

Axially chiral styrenes, which exhibit a chiral axis between a substituted alkene and an aromatic ring, have been largely overlooked. The hurdle is the lower barriers to rotation compared with that of their biaryl counterparts, rendering their asymmetric synthesis more difficult. We report herein the highly atroposelective synthesis via a C–H functionalization strategy of axially chiral styrenes with an open-chained alkene. Various axially chiral styrenes were produced by Pd(II)-catalyzed C–H alkenylation and alkynylation in good yields (up to 99%) and enantioselectivities (up to 99% ee) by using L-pyroglutamic acid as an inexpensive chiral ligand. The potent application of the styrene atropisomers is demonstrated by a Co(III)-catalyzed enantioselective C–H amidation of ferrocene with axially chiral styrene-type acid as chiral ligand. Experimental and computational studies were conducted to elucidate the reaction mechanism. The chiral induction model of the enantioselectivity-determining C–H bond activation step was also provided based on DFT calculations.

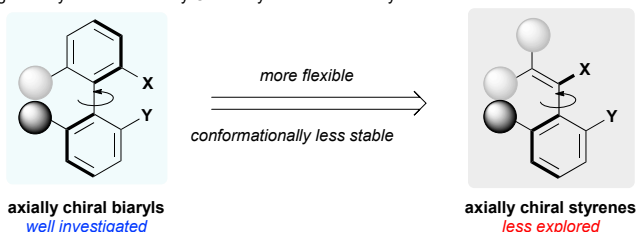
INTRODUCTION

Axially chiral compounds are ubiquitous in natural products and pharmaceuticals^{1,2} and have been widely used as versatile chiral ligands or catalysts in asymmetric synthesis.^{3–8} In distinct contrast to the well-investigated axially chiral biaryls,^{9–14} axially chiral styrenes, which exhibit a chiral axis between a substituted alkene and an aromatic ring have been largely overlooked,¹⁵ despite the fact that this type of axial chirality was realized and intensively studied by Adams and co-workers in the 1940s.¹⁶ The main hurdle is basically due to the flexible structure, which results in relatively lower barriers to rotation in comparison with their biaryl counterparts, rendering their asymmetric synthesis drastically more difficult (Scheme 1A).^{15,16} On the other hand, axially chiral styrenes have flourished gradually, as chiral olefins can not only be employed as synthons for total synthesis¹⁷ but also can be applied to asymmetric synthesis as chiral catalysts or ligands.^{18–20} Consequently, considerable efforts have been devoted to the development of efficient strategies for the asymmetric synthesis of the axially chiral styrene skeletons. In the early efforts, point-to-axial chirality transfer strategy has been reported by Baker,²¹ Hattori and Miyano,²² and Suzuki,¹⁷ employing stoichiometric chiral molecules with point chirality. Recently, more appealing catalytic asymmetric synthesis were achieved by the groups of Gu^{23,24} and Smith.²⁵ However, the scope of chiral styrenes were limited to arylcyclohexenes with the alkene skeleton trapped within a rigid ring to mimic the rigidity of biaryls and ensure the conformational stability. The situation becomes significantly more difficult when the targeted chiral styrene contains a chiral axis

The Bigger Picture

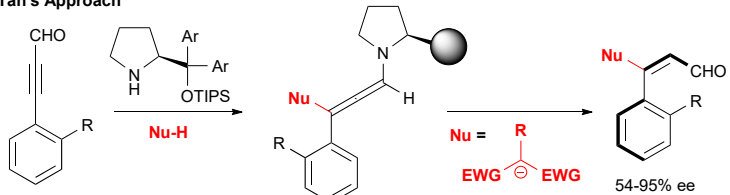
Atropisomerism, which stems from the hindered rotation around a chiral axis, is widely present in natural products, pharmaceuticals, and chiral catalysts or ligands. In contrast to the well-investigated biaryl atropisomers, the asymmetric synthesis of axially chiral styrenes bearing a chiral axis between an alkene and an aromatic ring remains a significant challenge. Here, we report a highly atroposelective synthesis of styrene atropisomers with open-chained alkene by asymmetric C–H functionalization by using available L-pyroglutamic acid as a chiral ligand. This strategy enables rapid access to a broad range of enantio-enriched axially chiral styrenes under mild conditions in an atom- and step-economical manner. The resulting axially chiral styrenes are important precursors for further elaborations, including the transformation into axially chiral styrene-type acids, which were demonstrated to be efficient chiral ligands in Co(III)-catalyzed enantioselective C–H amidation reactions.

A Challenges of Synthesis of Axially Chiral Styrenes with an Acyclic Alkenes

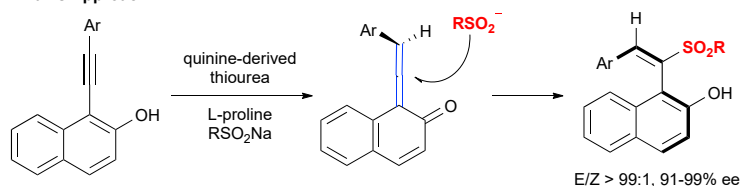


B Previous Strategy: Asymmetric Organocatalytic Addition

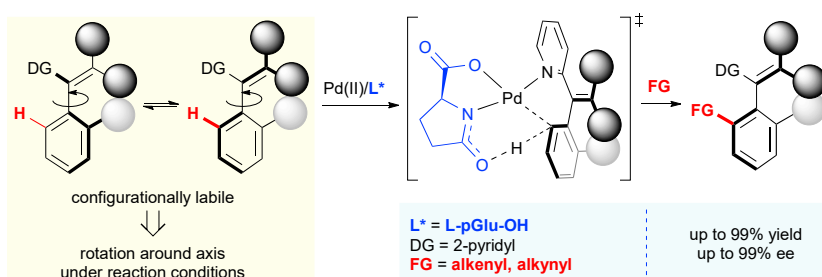
Tan's Approach



Yan's Approach



C Our Strategy: Asymmetric C–H Functionalization



Scheme 1. Challenges and Strategies for Construction of Axially Chiral Styrenes with an Acyclic Alkene

- (A) Challenges of synthesis of axially chiral styrenes with an acyclic alkene.
(B) Previous strategy: asymmetric organocatalytic addition by the groups of Tan and Yan.
(C) Our strategy: asymmetric C–H functionalization.

between an open-chained alkene and an aromatic ring. Thus far, only a single strategy involving asymmetric organocatalytic addition has been reported by the Tan²⁶ and Yan^{27,28} groups to access these axially chiral styrenes with an acyclic alkene (**Scheme 1B**). We speculated that an asymmetric C–H activation strategy involving the enantiospecific introduction of a bulky substituent at the *ortho*-position of the configurationally labile achiral compounds to lock the preformed axis would be an appealing approach.^{14,29–33} The success of this strategy would offer a straightforward way to access these synthetically challenging atropisomers in an atom- and step-economical manner (**Scheme 1C**).

Although asymmetric C–H functionalization has emerged as a powerful synthetic tool for the rapid generation of axially chiral biaryl skeletons,^{11,14,34–48} the

¹Department of Chemistry, Zhejiang University, Hangzhou 310027, China

²These authors contributed equally

³Lead Contact

*Correspondence: hxchem@zju.edu.cn (X.H.), bfshi@zju.edu.cn (B.-F.S.)

<https://doi.org/10.1016/j.chempr.2019.12.011>

construction of axially chiral styrenes bearing an open-chained alkene with more flexibility via catalytic asymmetric C–H functionalization remains elusive. At least two main difficulties needed to be addressed: first, the reaction has to be conducted under mild conditions in order to preserve enantiomeric purity of the resulting products because of the relatively lower conformational stability. Second, the judicious choice of a proper ligand and directing group (DG), which could cooperatively act to modulate the reactivity and effectively induce the enantioselectivity, is extremely challenging. Continuing with our long-standing efforts in construction of axial chirality via enantioselective C–H activation,^{43–48} we decided to tackle this synthetic challenge. Herein, we describe the highly atroposelective synthesis of axially chiral styrenes with open-chained alkene by Pd(II)-catalyzed atroposelective C–H alkenylation and alkynylation by using readily available L-pyroglutamic acid as a chiral ligand.

RESULTS AND DISCUSSION

Our initial investigations started with examining the reaction of styrene **1a** bearing a pyridyl DG with butyl acrylate (**2a**). In this system, interconversion between the corresponding atropoisomers of **1a** could occur easily while the resulting alkenylation product **3aa** is reasonably stable under elevated temperature typically employed in C–H activation reactions. Since the pioneering work by Yu and co-workers in 2008,⁴⁹ N-monoprotected α -amino acids (MPAAs) have been recognized as privileged chiral ligands for Pd(II)-catalyzed asymmetric C–H functionalization.^{49–53} Therefore, a variety of chiral carboxylic acids were tested first. To our delight, the desired alkenylation product **3aa** was obtained in 65% yield with 43% ee, when using L-pGlu-OH as ligand and AgOAc as oxidant in DCE (Table 1, entry 1).⁵⁴ After a survey of various solvents, we found that MeCN and MeOH could give promising results (entries 1–6). Encouraged by these results, a careful screening of a range of mixed solvents revealed that MeCN:^tBuOH (1:1, 0.05M) was the optimal solvent combination (entry 7, 93%, 89% ee). Further investigations of reaction temperature indicated that the well-designed model substrate is a good platform to test our hypothesis, as the alkenylation reaction could proceed at 50°C and both the reactivity and enantiocontrol were maintained (entry 8, 96%, 89% ee). Next, we evaluated the effect of silver salts, and Ag₃PO₄ was found to be the best oxidant (entry 13). The ee value could be improved to 95% without affecting the yield by further tuning the reaction concentration (entry 14). The use of Boc-L-pGlu-OH as ligand led to significantly low ee (entry 15, 21% ee). L-pGlu-OH was found to be the best ligand after a thorough evaluation of various chiral ligands, including spiro phosphoric acid, BINOL-derived phosphoric acid, BINOL, and other MPAAs (See Table S2 for details).

With the optimal reaction conditions in hand, we set out to explore the generality of the atroposelective C–H alkenylation (Scheme 2). Considering the low rotation barriers of axially chiral styrenes, 2,6-disubstitution is required to inhibit the rotation and epimerization. We first examined the steric effect in the *ortho*-position of the aromatic ring. Alkyl groups (**1b**, methyl; **1c**, ethyl; **1a**, isopropyl) and chloro (**1d**), were well-tolerated, giving high enantiocontrol (**3aa**–**3da**, 91%–96% ee). These experimental results are consistent with our computations that the alkenylation product bearing relatively larger substituent (R^1) leads to over 30 kcal/mol enantiomerization barrier (Figure S11). Substituents in the alkene terminus were also investigated. The replacement of dimethyl with diethyl or dipropyl in the alkene terminus is well-tolerated, giving the desired products in excellent yield and enantioselectivity (**3ea**, 99%, 92% ee; **3fa**, 95%, 93% ee). Cyclohexyl and cyclopentyl in the alkene terminus also gave high yield and good enantioselectivity (**3ga**, 99%, 91% ee; **3ha**, 87%, 95%

Table 1. Optimization of C–H Alkenylation

Entry	[Ag]	Solvent	T (°C)	Yield (%) ^a	ee (%) ^b
1	AgOAc	DCE	60	65	43
2	AgOAc	MeCN	60	90	79
3	AgOAc	1,4-dioxane	60	56	40
4	AgOAc	Toluene	60	85	25
5	AgOAc	MeOH	60	60	69
6	AgOAc	HFIP	60	85	-21
7	AgOAc	MeCN- ^t BuOH (1:1)	60	93	89
8	AgOAc	MeCN- ^t BuOH (1:1)	50	96	89
9	AgOAc	MeCN- ^t BuOH (1:1)	40	95	88
10	AgOAc	MeCN- ^t BuOH (1:1)	30	44	84
11	AgOAc	MeCN- ^t BuOH (4:1)	50	93	90
12	AgOAc	MeCN- ^t BuOH (4:1)	50	94	93
13	Ag ₂ SO ₄	MeCN- ^t BuOH (4:1)	50	93	94
14	Ag ₃ PO ₄	MeCN- ^t BuOH (4:1, 4 mL)	50	92 (85) ^c	95
15 ^d	Ag ₃ PO ₄	MeCN- ^t BuOH (4:1, 4 mL)	50	78	21

See also Table S1.^e

^aDetermined by ¹H NMR with CH₂Br₂ as the internal standard.

^bThe ee value was determined by chiral HPLC.

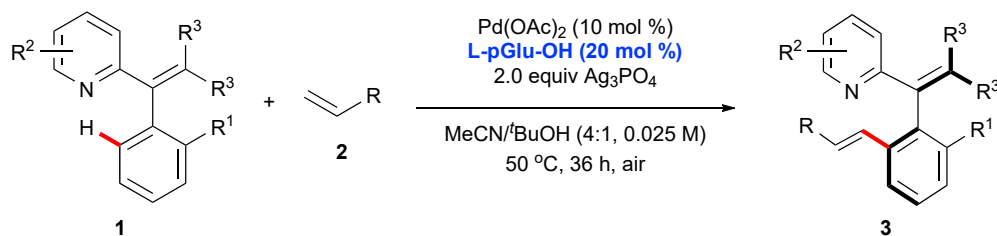
^cIsolated yield.

^dBoc-L-pGlu-OH.

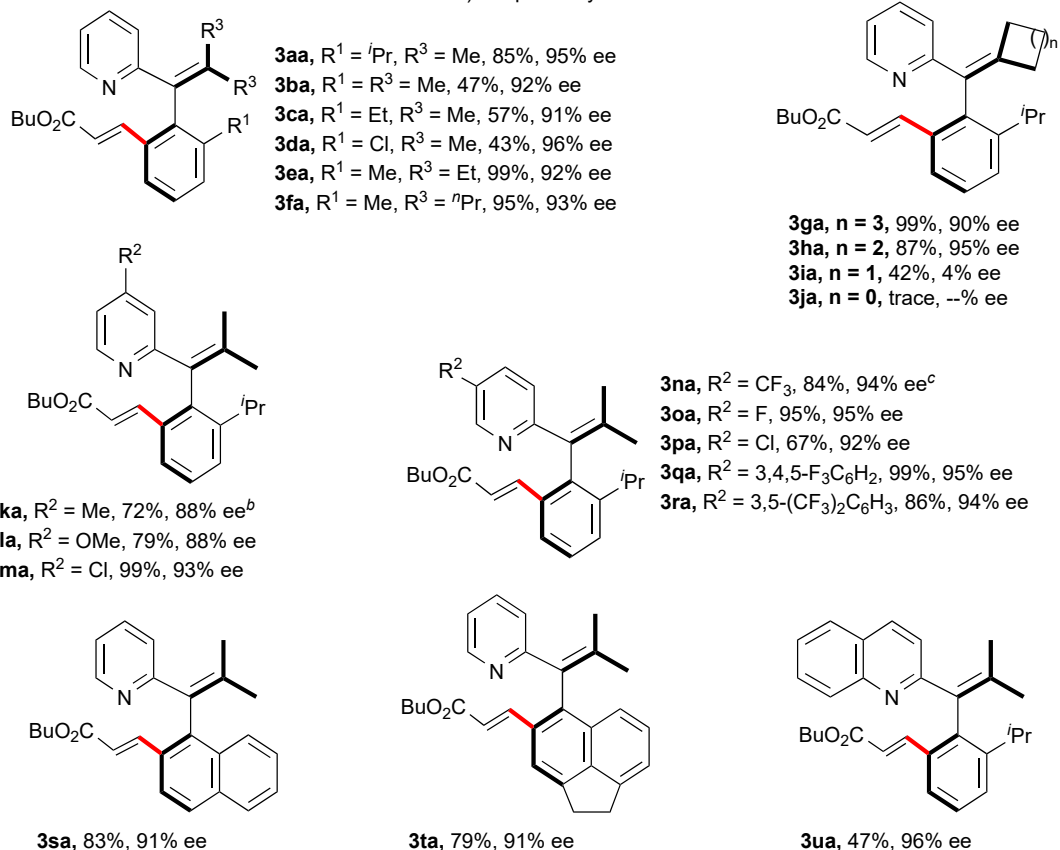
^e1a (0.1 mmol), 2a (2.0 equiv), Pd(OAc)₂ (10 mol %), [Ag] (2.0 equiv), L-pGlu-OH (20 mol %) in solvent (2 mL) at T °C for 36 h under air.

ee). However, small cyclic substituents, such as cyclobutyl and cyclopropyl resulted in significant loss of reactivity and enantioselectivity (3ia, 42%, 4% ee; 3ja, trace). The loss of reactivity could be explained by angle strain, which prevents the agostic interaction of palladium with the *ortho*-C–H bond in the aryl ring. Various substituents on the pyridyl ring were then tested, and we found that both electron-donating (1k, Me; 1l, OMe), halogen atoms (1m, 1p, Cl; 1o, F), trifluoromethyl (1n), and fluorinated aryl (1q and 1r) were all compatible with this reaction, affording the alkenylation products in high enantioselectivities (88%–95% ee). Naphthyl and 1,2-dihydroacenaphthyl type of substrates also showed good reactivity (3sa, 83%, 91% ee; 3ta, 79%, 91% ee). When a quinoline group was used as DG, the alkenylation product 3ua was obtained in excellent enantioselectivity (96% ee), albeit with moderate yield (47%).

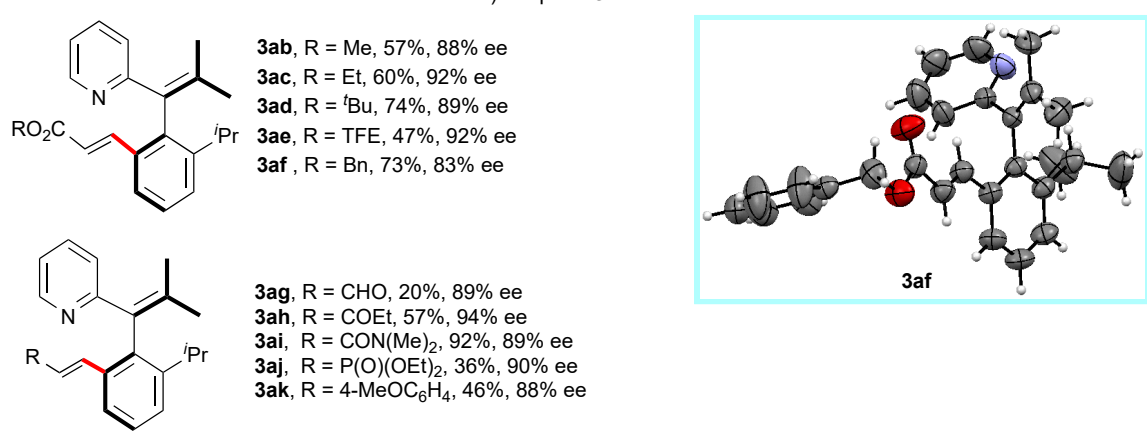
The generality of olefins was also investigated (Scheme 2B). Various acrylates were compatible with this reaction, giving the desired products in moderate to good yield and good enantioselectivities (3aa–3af). Besides, acrolein, vinyl ketone, acrylamide, alkenylphosphate, and 4-methoxystyrene, were all suitable partners and the corresponding axially chiral styrenes were afforded in good yields and enantioselectivities (3ag–3ak). The absolute configuration of products 3af was determined as R_a by X-ray



a) Scope of Styrenes



b) Scope of Olefins



Scheme 2. Scope of Pd(II)-catalyzed Atroposelective C–H Alkenylation

^a1 (0.1 mmol), 2 (2.0 equiv), Pd(OAc)₂ (10 mol %), Ag₃PO₄ (2.0 equiv), and L-pGlu-OH (20 mol %) in MeCN:tBuOH (4:1, 0.025 M) at 50°C for 36 h under air.

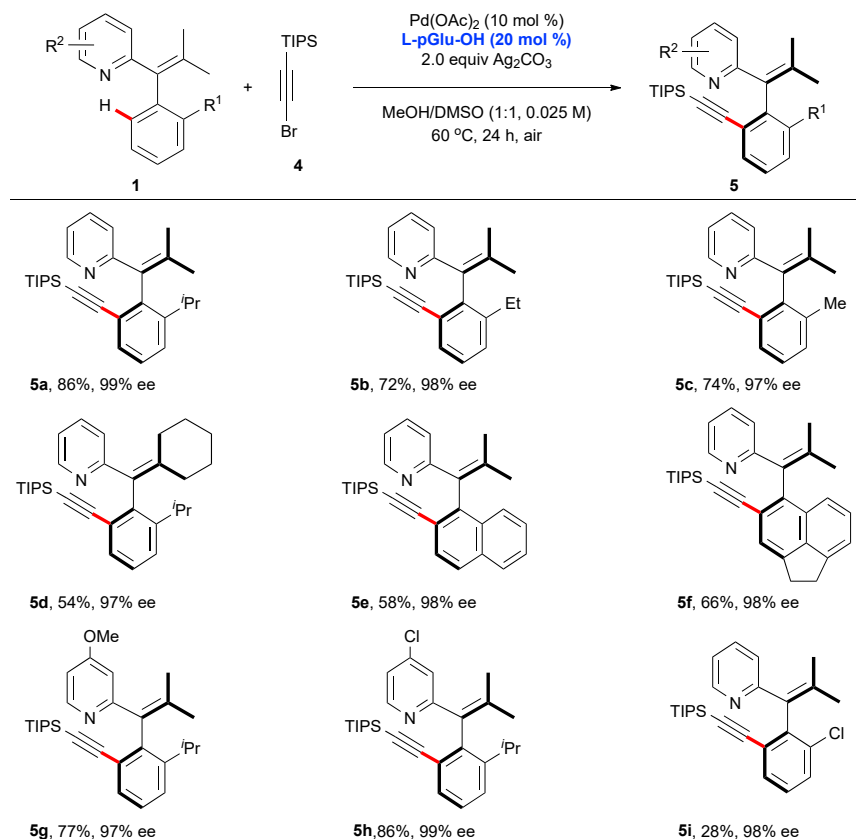
^bAg₂SO₄ (2.0 equiv).

^cAgOAc (2.0 equiv).

crystallographic analysis (see also *Figure S1*), and those of the others were assigned analogously.

These results prompted us to further investigate whether the strategy could be applied to other C–H functionalization reactions. We explored the asymmetric C–H alkynylation of **1a** with TIPS-protected alkynyl bromide **4** and found that the reaction proceeded efficiently under slightly modified conditions using L-pGlu-OH as chiral ligand (see *Table S2* for detailed optimizations). The desired alkylation product **5a** was finally obtained in 86% yield with 99% ee in the presence of 10 mol % Pd(OAc)₂, 20 mol % L-pGlu-OH, and 2.0 equiv of Ag₃PO₄ in MeOH:DMSO (1:1, 0.025 M) at 60°C for 24 h.

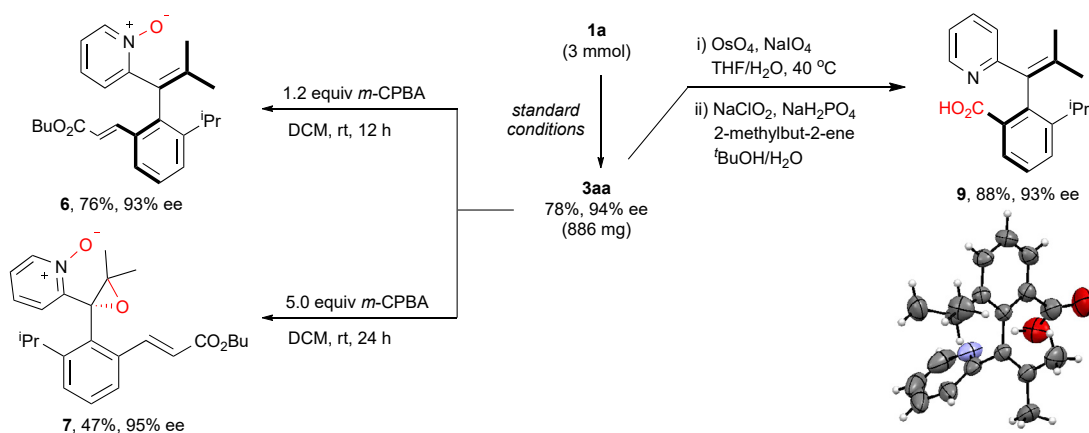
The scope of the C–H alkynylation was then examined with **4** as the coupling partner (*Scheme 3*). Generally, the atroposelective C–H alkynylation (**5a**–**5i**, 97%–99% ee) gave better enantiocontrol than the analogous C–H alkenylation (**3aa**–**3ea**, **3ga**–**3ha**, **3na**–**3oa**, 88%–96% ee).



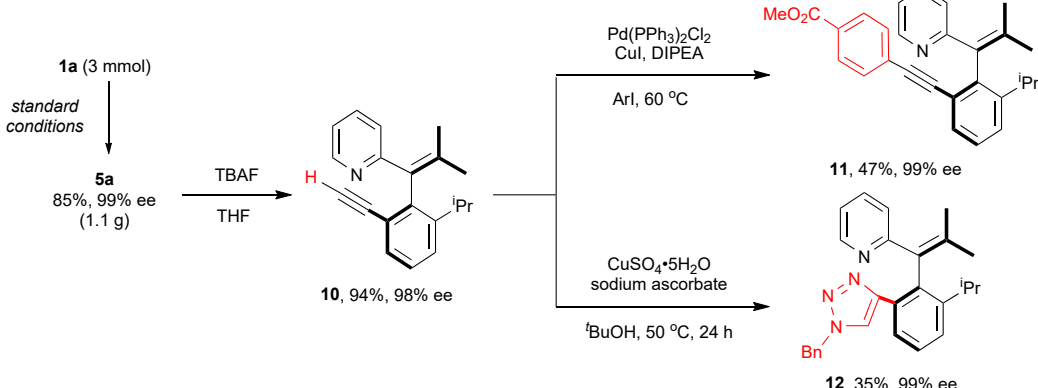
Scheme 3. Scope of Pd(II)-catalyzed Atroposelective C–H Alkynylation

^a1 (0.10 mmol), 4 (2.0 equiv), Pd(OAc)₂ (10 mol %), Ag₂CO₃ (2.0 equiv), L-pGlu-OH (20 mol %) in MeOH:DMSO (1:1, 0.025 M) at 60°C for 24 h under air.

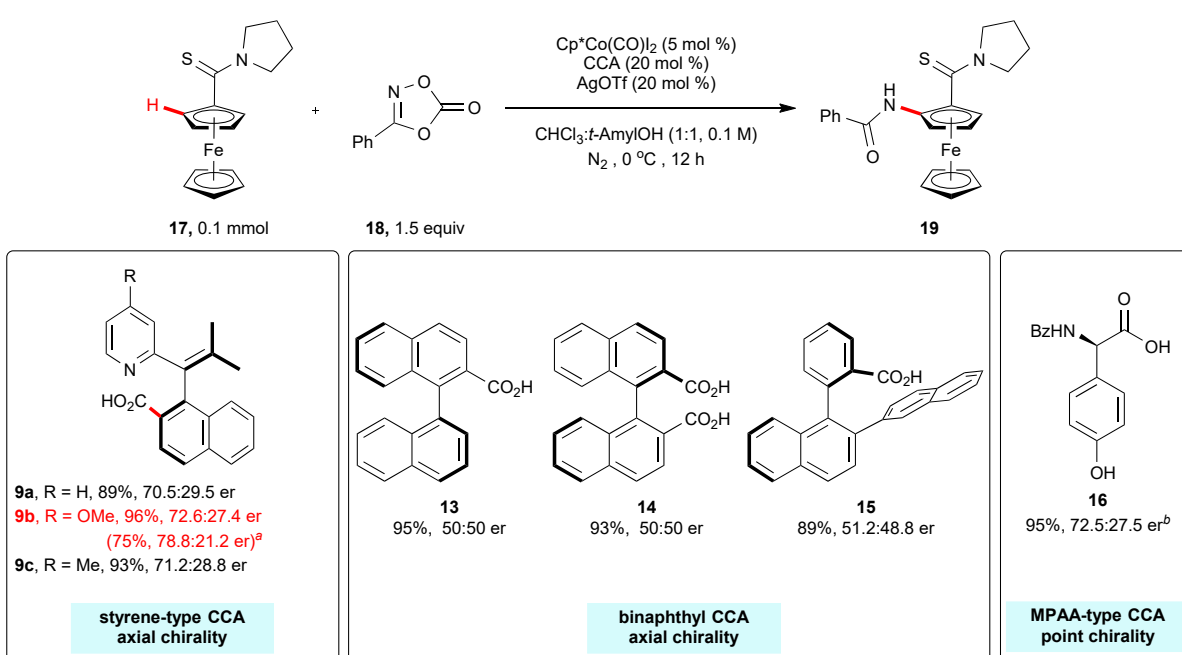
A Scale-up preparation of **3aa** and further elaboration



B Scale-up preparation of **5a** and further elaboration



C Application in Co(III)-catalyzed enantioselective C–H amination of ferrocene



Scheme 4. Scale-Up Preparation, Derivatization and Application

Please see the [Supplemental Information](#) for detailed experimental conditions (see also [Scheme S3](#)).

(A) Scale-up preparation of **3aa** and further elaborations.

(B) Scale-up preparation of **5a** and further elaborations.

(C) Application of chiral styrene atropisomers in Co(III)-catalyzed asymmetric C–H amination.^a–20°C.^bThe result was reported in Liu et al.⁵⁵

It should be noted that both of the C–H alkenylation and alkynylation reactions could be conducted on gram scale without the erosion of reactivity and enantioselectivity ([Scheme 4A](#), **3aa**, 886 mg, 78%, 94% ee; [Scheme 4B](#), **5a**, 1.1 g, 85%, 99% ee). Further derivatization of the resulting products was also conducted to showcase the synthetic potential. **3aa** could be oxidized to *N*-oxide pyridine derivative **6** with 1.2 equiv of *m*-CPBA in 76% yield with 93% ee. When the amount of *m*-CPBA was increased to 5.0 equiv, the epoxidation of the alkene at the chiral axis occurred smoothly, giving epoxide **7** in moderate yield and excellent enantioselectivity (47%, 95% ee). Notably, the axial chirality was completely transferred to the point chirality.

Moreover, the selective oxidative cleavage of the less hindered alkene with OsO₄/NaIO₄, followed by oxidation of the resulting aldehyde with NaClO₂, gave the axially chiral styrene-type carboxylic acid **9** in high yield and complete retention of chirality (88% yield for two steps, 93% ee). The absolute configuration of product **9** was also determined as *R*_a by X-ray crystallographic analysis (see also [Figure S2](#)). The alkynylation product **5a** could be desilylated to give the corresponding terminal alkyne **10** without the erosion of ee (94%, 98% ee). Subsequent Sonogashira coupling and copper-catalyzed alkyne-azide cycloaddition gave **11** and **12** in moderate yield and no erosion of enantioselectivity, respectively.

To demonstrate potential applications of these styrene atropisomers in asymmetric synthesis, we embarked to use the resulting axially chiral styrene-type acids **9** as chiral carboxylic acid (CCA) ligands in Co(III)-catalyzed enantioselective C–H amidation of ferrocenes ([Scheme 4C](#)).⁵⁵ In our previous study, the best result of enantioselective C–H amidation of thioamide **17** was achieved using D-N-benzoyl-*p*-hydroxyphenylglycine (Bz-Hpg-OH, **16**), a mono-protected α -amino acid (MPAA) with a point chirality, as chiral ligand (72.5:27.5 er).⁵⁵ We first attempted the use of **9a** as a chiral ligand and a comparable enantiocontrol was obtained (70.5:29.5 er). A preliminary screening of axially chiral acids (**9a**–**9c**) with different substituents on pyridine revealed that that axially chiral styrene-type acid **9b** with 4-methoxy substituted on pyridine gave better stereocontrol than that using Bz-Hpg-OH (**9b**, 78.8:21.2 er versus **16**, 72.5:27.5 er).⁵⁵ For comparison, axially chiral carboxylic acids possessing a binaphthyl or biaryl backbone either gave no enantiocontrol (**13** and **14**, racemic) or very low enantioselectivity (**15**, 51.2:48.8 er). These results showcase that the styrene atropisomers might be superior or complementary to axially chiral biaryl skeletons in certain asymmetric reactions.

A number of experiments were conducted to gain some preliminary insight into the mechanism. First, a linear correlation between the ee value of **3aa** and L-pGlu-OH was observed ([Figure S3](#)), indicating that a single L-pGlu-OH is involved in the stereo-determining step. Second, the kinetic isotope effect (KIE) was determined by comparing the initial reaction rate with H-1a to that with D-1a, the KIE values of 1.30 (without L-pGlu-OH) and 1.20 (with L-pGlu-OH) were obtained, respectively ([Figure 1A](#); see [Figures S2](#) and [S3](#) for details), indicating that C–H bond cleavage process might not be involved in a rate-determining step. Initial rate studies revealed a ligand deceleration effect (LDE) in this reaction ([Figure 1B](#);

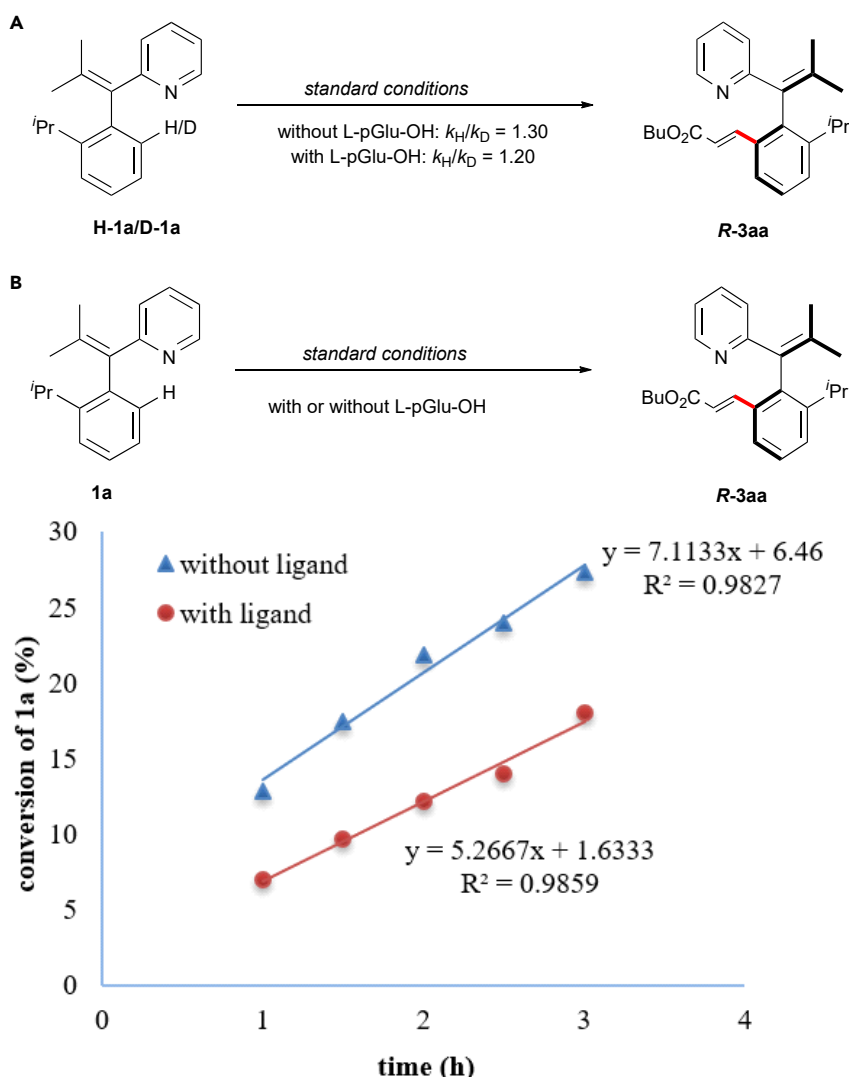


Figure 1. Mechanism Experiments

(A) KIE studies by comparing the initial rate with H-1a to that with D-1a (see Figures S4–S5 for details).

(B) Ligand effect on the reaction rate of atroposelective C–H alkenylation of 1a (see also Figure S6).

see Figure S14 for computational details). This is in sharp contrast to Pd-catalyzed atroposelective C–H alkenylation of biaryls using chiral spiro phosphoric acid ligands, in which the high enantioselectivity originated from a dramatic ligand acceleration effect.⁴⁷ LDE-induced highly enantioselective asymmetric synthesis is significantly more challenging than the accelerated scenario.⁵⁶ We rationalized that the high ee resulted from the suppression of background reaction by a highly favorable ligand exchange of L-pGlu-OH with Pd(OAc)₂ to form a chiral Pd(L-pGlu-O)(OAc)-type catalyst. This could also explain the need of excess of chiral ligand (2:1 ratio of ligand:palladium) to ensure that no uncomplexed palladium acetate is present.

We next explored the reaction mechanism and origins of enantioselectivity with density functional theory (DFT) calculations, using experimental styrene 1a and

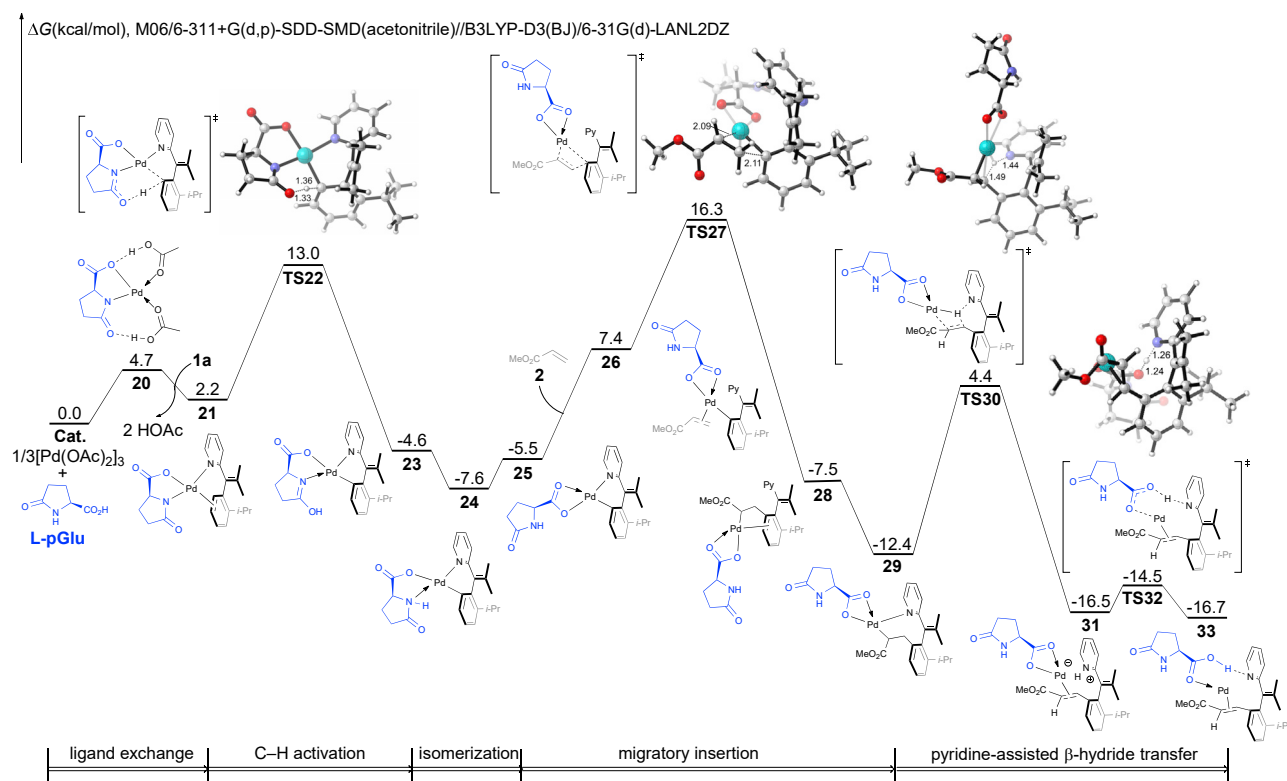


Figure 2. DFT-Computed Free-Energy Profile of the Most Favorable Pathway for the Pd/L-pGlu-Catalyzed Atroposelective C–H Alkenylation
See Figures S7–S9 for details.

methyl acrylate as the model compounds.⁵⁷ The DFT-computed free energy changes of the most favorable pathway for the Pd(II)/L-pGlu-catalyzed atroposelective C–H alkenylation are shown in Figure 2 (see the *Supplemental Information* for details). The Pd(OAc)₂ trimer first deprotonates the amino acid L-pGlu, generating the intermediate 20. Subsequent complexation with styrene 1a leads to the intermediate 21, which undergoes the concerted metalation-deprotonation via TS22 to produce the aryl-palladium species 23. 23 isomerizes to the more stable 25 to allow the alkene insertion via TS27.⁵⁸ This alkene insertion generates the alkyl-palladium species 28. 28 isomerizes to the more stable 29 with pyridine coordination, followed by the pyridine-assisted β-hydride transfer,^{59–61} through TS30. Subsequent proton transfer from pyridinium to carboxylate via TS32 produces the product-coordinated complex 33. This pyridine-assisted β-hydride transfer process is significantly more favorable than the alternative β-hydride elimination involving palladium-hydride species and carboxylate-assisted β-hydride transfer (Figures S8 and S9). Based on the computed free energy profile, the on-cycle resting state is the aryl-palladium species 24. The rate-determining step is the alkene insertion via TS27, which requires an overall barrier of 23.9 kcal/mol comparing with the resting state 24. The facile C–H bond activation is consistent with the KIE experimental results.

To reveal the origins of enantioselectivity, DFT calculations of the enantioisomeric product-formation pathways were conducted (Figure 3). The formation of the major enantiomer (black pathway) involves a reversible C–H bond activation via TS22 and the subsequent rate-determining alkene insertion via TS27. The

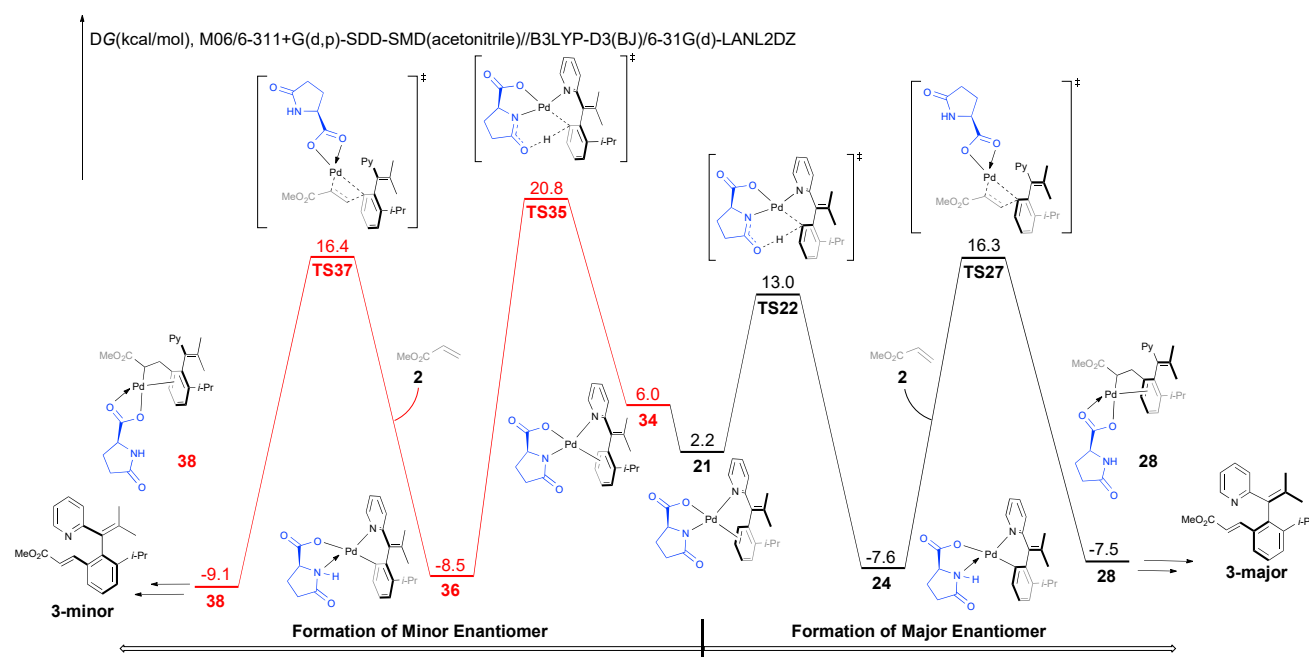


Figure 3. DFT-Computed Free-Energy Changes of the Enantioisomeric Pathways in the Pd/L-pGlu-Catalyzed Atroposelective C–H Alkenylation
Free energies are compared to separate $[Pd(OAc)_3]$ and ligands (see also Figure S13).

competing formation of the minor enantiomer (red pathway) is inhibited by the C–H bond activation step via TS35.⁶² Comparing the determining steps (TS27 versus TS35), the formation of the major enantiomer is 4.5 kcal/mol more favorable than that of the minor enantiomer, which corroborated the excellent enantioselectivities in experimental observations. The dramatic energy difference between the C–H bond activation transition states (TS22 versus TS35) is the key reason that differentiates the enantioisomeric pathways. We also confirmed that the racemization of axial chirality is not feasible after the C–H bond activation step (Figure S10). The alkenyl tether is not related to the enantioselectivity control (Figures 4A and 4B); replacing the alkenyl tether (TS22 versus TS35) with a simple methylene unit (TS39 versus TS40) also leads to excellent chiral discrimination in the C–H bond activation step. The analysis of the chiral induction of C–H bond activation step is included in Figure 4C. The model transition state TS41 for the C–H bond activation of benzene suggested that the chiral amino acid intrinsically prefers to have the C–H bond activation occurring in the third quadrant. This chiral induction nicely matches the axial chirality of the C–H bond activation via TS22 for the major product-formation pathway. TS22 does not require significant distortion of amino acid ligand. The sp^3 -hybridized nitrogen of amino acid in TS22 has a similar pyramidalization geometry as compared to that in TS41, as reflected in the highlighted pyramidalization⁶³ at nitrogen. In contrast, the disfavored C–H bond activation transition state TS35 has a chiral mismatch between the amino acid ligand and the axial chirality of styrene. This forces the significant distortion of the amino acid ligand in TS35. The pyramidalization angle of the amino acid nitrogen is only 4.7° . We further computed the energy difference of the Pd(L-pGlu) fragment in the competing transition states. The 5.6 kcal/mol energy difference corroborated the rationale that the amino acid ligand distortion controls the enantioselectivity in the C–H bond activation step.

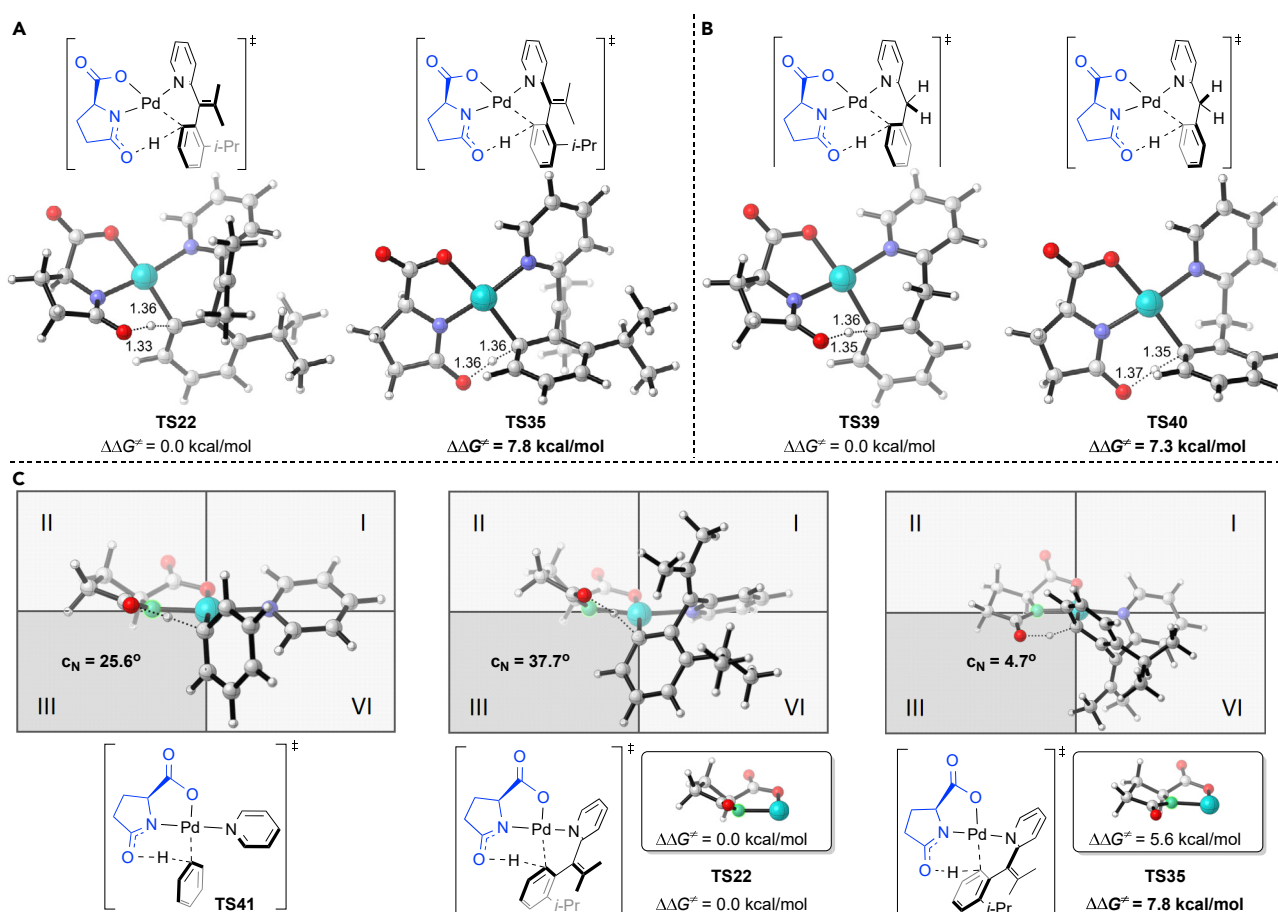


Figure 4. Computational Details

(A) Origins of enantioselectivity in the Pd/L-pGlu-catalyzed atroposelective C–H alkenylation.
(B) Tether effect on the enantioselectivity.
(C) Chiral induction through ligand distortion. For computational details, see the [Supplemental Information](#).

Conclusions

In summary, we have developed a Pd(II)/L-pGlu-OH catalytic system to enable the synthesis of axially chiral styrenes with an open-chained alkene via atroposelective C–H alkenylation and alkynylation, which significantly expands the synthetic toolkit for the accessing this family of atropoisomers. Experimental and computational studies were conducted to elucidate the reaction mechanism of atroposelective C–H alkenylation, which involves sequential C–H bond activation, alkene insertion, and pyridine-assisted β-hydride transfer. The chiral induction model of the enantioselectivity-determining C–H bond activation step was also provided based on DFT calculations. We expect that the newly developed asymmetric C–H functionalization strategy would streamline access to chiral styrenes. The use of commercially available L-pGlu-OH as a uniquely effective chiral ligand might also offer great opportunities in enantioselective C–H activation.

EXPERIMENTAL PROCEDURES

Full experimental procedures are provided in the [Supplemental Information](#).

See [Schemes S1–S3; Figures S1–S267](#) for synthesis and characterization of all new compounds.

DATA AND CODE AVAILABILITY

The crystallography data have been deposited at the Cambridge Crystallographic Data Center (CCDC) under accession number CCDC: 1907624 (3af), 1907625 (9) and can be obtained free of charge from www.ccdc.cam.ac.uk/getstructures.

SUPPLEMENTAL INFORMATION

Supplemental Information can be found online at <https://doi.org/10.1016/j.chempr.2019.12.011>.

ACKNOWLEDGMENTS

Financial support from the NSFC (21772170 and 21572201 for B.-F.S.) and (21702182 and 21873081 for X.H.), Outstanding Young Talents of Zhejiang Province High-level Personnel of Special Support (ZJWR0108 for B.-F.S.), the Fundamental Research Funds for the Central Universities (2018XZZX001-02 for B.-F.S. and 2019QNA3009 for X.H.), and Zhejiang Provincial NSFC (LR17B020001 for B.-F.S.) is gratefully acknowledged.

AUTHOR CONTRIBUTIONS

B.-F.S., L.J., and Q.-J.Y. conceived and designed the study. B.-F.S., X.H., L.J., and P.-P.X. co-wrote the paper. X.H. and P.-P.X. provided the density functional theory (DFT) calculations. L.J., Q.-J.Y., Y.L., B.-B.Z., and Y.-Q.H. performed the experiments and analyzed the data.

DECLARATION OF INTERESTS

The authors declare no competing interests.

Received: July 23, 2019

Revised: November 5, 2019

Accepted: December 10, 2019

Published: January 9, 2020

REFERENCES

1. Smyth, J.E., Butler, N.M., and Keller, P.A. (2015). A twist of nature – the significance of atropisomers in biological systems. *Nat. Prod. Rep.* 32, 1562–1583.
2. Clayden, J., Moran, W.J., Edwards, P.J., and LaPlante, S.R. (2009). The challenge of atropisomerism in drug discovery. *Angew. Chem. Int. Ed. Engl.* 48, 6398–6401.
3. Noyori, R., and Takaya, H. (1990). BINAP: an efficient chiral element for asymmetric catalysis. *Acc. Chem. Res.* 23, 345–350.
4. Chen, Y., Yekta, S., and Yudin, A.K. (2003). Modified BINOL ligands in asymmetric catalysis. *Chem. Rev.* 103, 3155–3212.
5. Brunel, J.M. (2007). Update 1 of: BINOL: a versatile chiral reagent. *Chem. Rev.* 107, PR1–PR45.
6. Q.-L. Zhou, ed. (2011). *Privileged Chiral Ligands and Catalysts* (Wiley-VCH Press).
7. Parmar, D., Sugiono, E., Raja, S., and Rueping, M. (2014). Complete field guide to asymmetric BINOL-phosphate derived Brønsted acid and metal catalysis: history and classification by mode of activation; Brønsted acidity, hydrogen bonding, ion pairing, and metal phosphates. *Chem. Rev.* 114, 9047–9153.
8. Akiyama, T., and Mori, K. (2015). Stronger Brønsted acids: recent progress. *Chem. Rev.* 115, 9277–9306.
9. Baudoin, O. (2005). The asymmetric Suzuki coupling route to axially chiral biaryls. *Eur. J. Org. Chem.* 2005, 4223–4229.
10. Bringmann, G., Price Mortimer, A.J., Keller, P.A., Gresser, M.J., Garner, J., and Breuning, M. (2005). Atroposelective synthesis of axially chiral biaryl compounds. *Angew. Chem. Int. Ed. Engl.* 44, 5384–5427.
11. Wencel-Delord, J., Panossian, A., Leroux, F.R., and Colobert, F. (2015). Recent advances and new concepts for the synthesis of axially stereoenriched biaryls. *Chem. Soc. Rev.* 44, 3418–3430.
12. Wang, Y.B., and Tan, B. (2018). Construction of axially chiral compounds via asymmetric organocatalysis. *Acc. Chem. Res.* 51, 534–547.
13. Link, A., and Sparr, C. (2018). Stereoselective arene formation. *Chem. Soc. Rev.* 47, 3804–3815.
14. Liao, G., Zhou, T., Yao, Q.-J., and Shi, B.-F. (2019). Recent advance in the synthesis of axially chiral biaryls via transition metal-catalysed asymmetric C–H functionalization. *Chem. Commun.* 55, 8514–8523.
15. Kumarasamy, E., Raghunathan, R., Sibi, M.P., and Sivaguru, J. (2015). Nonbiaryl and Heterobiaryl atropisomers: molecular templates with promise for Atroposelective chemical transformations. *Chem. Rev.* 115, 11239–11300.

16. Adams, R., and Miller, M.W. (1940). Restricted rotation in aryl olefins. I. preparation and resolution of β -chloro- β -(2,4,6-trimethyl-3-bromophenyl)- α -methylacrylic Acid. *J. Am. Chem. Soc.* 62, 53–56.
17. Mori, K., Ohmori, K., and Suzuki, K. (2009). Stereochemical relay via axially chiral styrenes: asymmetric synthesis of the antibiotic TAN-1085. *Angew. Chem. Int. Ed. Engl.* 48, 5633–5637.
18. Defieber, C., Grützmacher, H., and Carreira, E.M. (2008). Chiral olefins as steering ligands in asymmetric catalysis. *Angew. Chem. Int. Ed. Engl.* 47, 4482–4502.
19. Dong, H.-Q., Xu, M.-H., Feng, C.-G., Sun, X.-W., and Lin, G.-Q. (2015). Recent applications of chiral N-tert-butanesulfinyl imines, chiral diene ligands and chiral sulfur-olefin ligands in asymmetric synthesis. *Org. Chem. Front* 2, 73–89.
20. Nagamoto, M., and Nishimura, T. (2017). Asymmetric transformations over iridium/chiral diene catalysis. *ACS Catal* 7, 833–847.
21. Baker, R.W., Hambley, T.W., Turner, P., and Wallace, B.J. (1996). Central to axial chirality transfer via double bond migration: asymmetric synthesis and determination of the absolute configuration of axially chiral 1-(3'-indenyl)naphthalenes. *Chem. Commun.* 2571, 2571–2572.
22. Hattori, T., Date, M., Sakurai, K., Morohashi, N., Kosugi, H., and Miyano, S. (2001). Highly stereospecific conversion of C-entreochirality of a 3,4-dihydro-2H-1,1'-binaphthalen-1-ol into axial chirality of a 3,4-dihydro-1,1'-binaphthalene. *Tetrahedron Lett.* 42, 8035–8038.
23. Feng, J., Li, B., He, Y., and Gu, Z.-H. (2016). Enantioselective synthesis of atropisomeric vinyl arene compounds by palladium catalysis: a carbene strategy. *Angew. Chem. Int. Ed. Engl.* 55, 2186–2190.
24. Pan, C., Zhu, Z., Zhang, M., and Gu, Z.-H. (2017). Palladium-catalyzed enantioselective synthesis of 2-aryl cyclohex-2-enone atropisomers: platform molecules for the divergent synthesis of axially chiral biaryl compounds. *Angew. Chem. Int. Ed. Engl.* 56, 4777–4781.
25. Jolliffe, J.D., Armstrong, R.J., and Smith, M.D. (2017). Catalytic enantioselective synthesis of atropisomeric biaryls by a cation-directed O-alkylation. *Nat. Chem.* 9, 558–562.
26. Zheng, S.C., Wu, S., Zhou, Q., Chung, L.W., Ye, L., and Tan, B. (2017). Organocatalytic atroposelective synthesis of axially chiral styrenes. *Nat. Commun.* 8, 15238.
27. Jia, S., Chen, Z., Zhang, N., Tan, Y., Liu, Y., Deng, J., and Yan, H.-L. (2018). Organocatalytic enantioselective construction of axially chiral sulfone-containing styrenes. *J. Am. Chem. Soc.* 140, 7056–7060.
28. Tan, Y., Jia, S.-Q., Hu, F.-L., Liu, Y.-D., Peng, L., Li, D.-M., and Yan, H.-L. (2018). Enantioselective construction of vicinal diaxial styrenes and multiaxis system via organocatalysis. *J. Am. Chem. Soc.* 140, 16893–16898.
29. Wencel-Delord, J., and Colobert, F. (2013). Asymmetric C(sp²)-H Activation. *Chem. Eur. J.* 19, 14010–14017.
30. Zheng, C., and You, S.-L. (2014). Recent development of direct asymmetric functionalization of inert C–H bonds. *RSC Adv* 4, 6173.
31. Gao, D.-W., Zheng, J., Ye, K.-Y., Zheng, C., and You, S.-L. (2015). In *Asymmetric Functionalization of C–H Bonds*, S.-L. You, ed. (Royal Society of Chemistry), p. 141.
32. Newton, C.G., Wang, S.G., Oliveira, C.C., and Cramer, N. (2017). Catalytic enantioselective transformations involving C–H Bond cleavage by transition-metal complexes. *Chem. Rev.* 117, 8908–8976.
33. Saint-Denis, T.G., Zhu, R.Y., Chen, G., Wu, Q.F., and Yu, J.Q. (2018). Enantioselective C(sp³)-H bond activation by chiral transition metal catalysts. *Science* 359, 759.
34. Zheng, J., and You, S.L. (2014). Construction of axial chirality by rhodium-catalyzed asymmetric dehydrogenative Heck coupling of biaryl compounds with alkenes. *Angew. Chem. Int. Ed. Engl.* 53, 13244–13247.
35. Gao, D.-W., Gu, Q., and You, S.-L. (2014). Pd(II)-catalyzed intermolecular direct C–H Bond iodination: an efficient approach toward the synthesis of axially chiral compounds via kinetic resolution. *ACS Catal* 4, 2741–2745.
36. Wang, Q., Cai, Z.J., Liu, C.X., Gu, Q., and You, S.L. (2019). Rhodium-catalyzed atroposelective C–H arylation: efficient synthesis of axially chiral Heterobiaryls. *J. Am. Chem. Soc.* 141, 9504–9510.
37. Hazra, C.K., Dherbassy, Q., Wencel-Delord, J., and Colobert, F. (2014). Synthesis of axially chiral biaryls through sulfoxide-directed asymmetric mild C–H activation and dynamic kinetic resolution. *Angew. Chem. Int. Ed. Engl.* 53, 13871–13875.
38. He, C., Hou, M., Zhu, Z., and Gu, Z.-H. (2017). Enantioselective synthesis of indole-based biaryl atropisomers via palladium-catalyzed dynamic kinetic intramolecular C–H cyclization. *ACS Catal* 7, 5316–5320.
39. Jia, Z.J., Merten, C., Gontla, R., Daniliuc, C.G., Antonchick, A.P., and Waldmann, H. (2017). General enantioselective C–H activation with efficiently tunable cyclopentadienyl ligands. *Angew. Chem. Int. Ed. Engl.* 56, 2429–2434.
40. Newton, C.G., Braconi, E., Kuziola, J., Wodrich, M.D., and Cramer, N. (2018). Axially chiral Dibenzazepinones by a palladium(0)-catalyzed atropo-enantioselective C–H arylation. *Angew. Chem. Int. Ed. Engl.* 57, 11040–11044.
41. Jang, Y.-S., Woźniak, Ł., Pedroni, J., and Cramer, N. (2018). Access to P- and axially chiral biaryl phosphine oxides by enantioselective CpxIrIII-catalyzed C–H arylations. *Angew. Chem. Int. Ed. Engl.* 57, 12901–12905.
42. Tian, M.-M., Bai, D., Zheng, G.-F., Chang, J.-B., and Li, X.-W. (2019). Rh(III)-catalyzed asymmetric synthesis of axially chiral Biindolyls by merging C–H activation and nucleophilic Cy-cyclization. *J. Am. Chem. Soc.* 141, 9527–9532.
43. Yao, Q.J., Zhang, S., Zhan, B.B., and Shi, B.F. (2017). Atroposelective synthesis of axially chiral biaryls by palladium-catalyzed asymmetric C–H olefination enabled by a transient chiral auxiliary. *Angew. Chem. Int. Ed. Engl.* 56, 6617–6621.
44. Liao, G., Yao, Q.J., Zhang, Z.Z., Wu, Y.J., Huang, D.Y., and Shi, B.F. (2018). Scalable, stereocontrolled formal syntheses of (+)-Isoschizandrin and (+)-Steganone: development and applications of palladium(II)-catalyzed atroposelective C–H alkynylation. *Angew. Chem. Int. Ed. Engl.* 57, 3661–3665.
45. Liao, G., Li, B., Chen, H.M., Yao, Q.J., Xia, Y.N., Luo, J., and Shi, B.F. (2018). Pd-Catalyzed atroposelective C–H allylation through β -O elimination: diverse synthesis of axially chiral biaryls. *Angew. Chem. Int. Ed. Engl.* 57, 17151–17155.
46. Zhang, S., Yao, Q.-J., Liao, G., Li, X., Li, H., Chen, H.-M., Hong, X., and Shi, B.-F. (2019). Enantioselective synthesis of atropisomers featuring pentatomic heteroaromatics by Pd-catalyzed C–H alkynylation. *ACS Catal* 9, 1956–1961.
47. Luo, J., Zhang, T., Wang, L., Liao, G., Yao, Q.-J., Wu, Y.-J., Zhan, B.-B., Lan, Y., Lin, X.-F., and Shi, B.-F. (2019). Enantioselective synthesis of biaryl atropisomers via Pd-catalyzed C–H olefination using chiral spiro phosphoric acid ligands. *Angew. Chem. Int. Ed. Engl.* 58, 6708–6712.
48. Liao, G., Chen, H.-M., Xia, Y.-N., Li, B., Yao, Q.-J., and Shi, B.-F. (2019). Synthesis of chiral aldehyde catalysts via Pd-catalyzed atroposelective C–H Naphthylation. *Angew. Chem. Int. Ed. Engl.* 58, 11464–11468.
49. Shi, B.-F., Maugel, N., Zhang, Y.-H., and Yu, J.-Q. (2008). Pd(II)-catalyzed enantioselective activation of C(sp²)-H and C(sp³)-H bonds using monoprotected amino acids as chiral ligands. *Angew. Chem. Int. Ed. Engl.* 47, 4882–4886.
50. Shi, B.-F., Zhang, Y.-H., Lam, J.K., Wang, D.H., and Yu, J.Q. (2010). Pd(II)-catalyzed enantioselective C–H olefination of diphenylacetic acids. *J. Am. Chem. Soc.* 132, 460–461.
51. Wasa, M., Engle, K.M., Lin, D.W., Yoo, E.J., and Yu, J.Q. (2011). Pd(II)-catalyzed enantioselective C–H activation of cyclopropanes. *J. Am. Chem. Soc.* 133, 19598–19601.
52. Gao, D.W., Shi, Y.C., Gu, Q., Zhao, Z.L., and You, S.L. (2013). Enantioselective synthesis of planar chiral ferrocenes via palladium-catalyzed direct coupling with arylboronic acids. *J. Am. Chem. Soc.* 135, 86–89.
53. Engle, K.M. (2016). The mechanism of palladium(II)-mediated C–H cleavage with Mono-N-protected amino acid (MPAA) ligands: origins of rate acceleration. *Pure Appl. Chem.* 88, 119–138.
54. Han, H., Zhang, T., Yang, S.D., Lan, Y., and Xia, J.B. (2019). Palladium-catalyzed enantioselective C–H aminocarbonylation: synthesis of

- chiral isoquinolinones. *Org. Lett.* **21**, 1749–1754.
55. Liu, Y.H., Li, P.X., Yao, Q.J., Zhang, Z.Z., Huang, D.Y., Le, M.D., Song, H., Liu, L., and Shi, B.F. (2019). Cp^{*}Co(III)/MPAA-catalyzed enantioselective amidation of ferrocenes directed by thioamides under mild conditions. *Org. Lett.* **21**, 1895–1899.
56. Fundamentals of Asymmetric Catalysis. (2008), P.J. Walsh and M.C. Kozlowski, eds. (University Science Books).
57. Computations were performed with Gaussian 09 software package. Computational details are included in the Supplemental Information.
58. Various forms of the coordinating amino acid were considered for the rate-determining alkene insertion, details are included in the Supplemental Information (Figure S7).
59. Noda, S., Nakamura, A., Kochi, T., Chung, L.W., Morokuma, K., and Nozaki, K. (2009). Mechanistic studies on the formation of linear polyethylene chain catalyzed by palladium phosphine-sulfonate complexes: experiment and theoretical studies. *J. Am. Chem. Soc.* **131**, 14088–14100.
60. Hong, X., Wang, J., Yang, Y.-F., He, L., Ho, C.-Y., and Houk, K.N. (2015). Computational exploration of mechanism and selectivities of (NHC) nickel(II)hydride-catalyzed hydroalkenylations of styrene with α -olefins. *ACS Catal.* **5**, 5545–5555.
61. Xiao, L.J., Zhao, C.Y., Cheng, L., Feng, B.Y., Feng, W.M., Xie, J.H., Xu, X.F., and Zhou, Q.L. (2018). Nickel(0)-catalyzed hydroalkenylation of imines with styrene and its derivatives. *Angew. Chem. Int. Ed. Engl.* **57**, 3396–3400.
62. The full energy profile of the minor enantiomer formation is included in the Supplemental Information (Figure S13).
63. Szostak, M., and Aubé, J. (2013). Chemistry of bridged lactams and related heterocycles. *Chem. Rev.* **113**, 5701–5765.